

# Decay scheme of $^{50}\text{V}$

F.A. Danevich<sup>a,1</sup>, M. Hult<sup>b</sup>, D.V. Kasperovych<sup>a</sup>, V.R. Klavdiienko<sup>a</sup>, G. Lutter<sup>b</sup>,  
G. Marissens<sup>b</sup>, O.G. Polischuk<sup>a</sup>, V.I. Tretyak<sup>a</sup>

<sup>a</sup>*Institute for Nuclear Research of NASU, 03028 Kyiv, Ukraine*

<sup>b</sup>*European Commission, Joint Research Centre, Retieseweg 111, 2440 Geel, Belgium*

## Abstract

Investigation of the  $^{50}\text{V}$  electron-capture to the  $2^+$  1553.8 keV level of  $^{50}\text{Ti}$  and search for  $\beta^-$  decay of  $^{50}\text{V}$  to the  $2^+$  783.3 keV level of  $^{50}\text{Cr}$  (both those decays are fourfold forbidden with  $\Delta J^{\Delta\pi} = 4^+$ ) have been performed using a vanadium sample of natural isotopic abundance with mass of 955 g. The measurements were conducted with the help of an ultra low-background HPGe-detector system located 225 m underground in the laboratory HADES (Belgium). The measured value of the half-life of  $^{50}\text{V}$  for electron capture was  $T_{1/2}^{\text{EC}} = (2.77^{+0.20}_{-0.19}) \times 10^{17}$  yr. The  $\beta^-$ -decay branch was not detected and the corresponding lower bound of the half-life was  $T_{1/2}^{\beta} \geq 8.9 \times 10^{18}$  yr at the 90% confidence level.

*Keywords:*  $^{50}\text{V}$ ; Electron capture; Beta decay; Low-background HPGe  $\gamma$  spectrometry

## 1 INTRODUCTION

The isotope  $^{50}\text{V}$  is present in the natural mixture of vanadium with a very low abundance of 0.250(10)% [1]. Taking into account the mass difference between  $^{50}\text{V}$  and  $^{50}\text{Ti}$  ( $2207.6 \pm 0.4$  keV [2]), and between  $^{50}\text{V}$  and  $^{50}\text{Cr}$  ( $1038.06 \pm 0.30$  keV [2]), both electron capture (EC) of  $^{50}\text{V}$  to  $^{50}\text{Ti}$  and  $\beta^-$  decay of  $^{50}\text{V}$  to  $^{50}\text{Cr}$  are possible (the decay scheme of  $^{50}\text{V}$  is shown in Fig. 1). However, decays of  $^{50}\text{V}$  to the ground states of  $^{50}\text{Ti}$  and  $^{50}\text{Cr}$  are strongly suppressed by the very large spin change  $\Delta J = 6$  in both the cases. The only excited levels on which decay of  $^{50}\text{V}$  can undergo are the  $2^+$  1553.8 keV level of  $^{50}\text{Ti}$ , and the  $2^+$  783.3 keV level of  $^{50}\text{Cr}$ . Both the decay channels are fourfold forbidden non-unique ( $\Delta J^{\Delta\pi} = 4^+$ ). Since in both channels decay goes to the excited levels of daughter nuclei, de-excitation  $\gamma$ -ray quanta can be detected by  $\gamma$  spectrometry of a vanadium sample. While the  $^{50}\text{V}$  electron-capture transition to the  $2^+$  1553.8 keV level of  $^{50}\text{Ti}$  is observed in several experiments, the  $\beta^-$  decay of  $^{50}\text{V}$  to the  $2^+$  783.3 keV level of  $^{50}\text{Cr}$  remains unobserved (despite two claims of detection that have been disproved in the subsequent more sensitive investigations). The history of  $^{50}\text{V}$  decays investigations is summarized in Table 1 (see also recent review [15]).

The decay of  $^{50}\text{V}$  is of especial interest since the transitions involve several different nuclear matrix elements with the associated different phase-space factors multiplied by the axial-vector

---

<sup>1</sup>Corresponding author. *E-mail address:* danevich@kinr.kiev.ua (F.A. Danevich).

coupling constant  $g_A$  [16]. This constant plays an important role in the neutrinoless double  $\beta$  decay probability calculations [17, 18, 19, 20, 21]. Recent calculations in nuclear shell model [16] result in the following (partial) half-lives for the two decay modes:  $T_{1/2}^{\text{EC}} = (5.13 \pm 0.07)[(3.63 \pm 0.05)] \times 10^{17}$  yr given for  $g_A = 1.00[1.25]$ ; for the  $\beta^-$ -decay branch,  $T_{1/2}^{\beta} = (2.34 \pm 0.02)[(2.00 \pm 0.02)] \times 10^{19}$  yr.

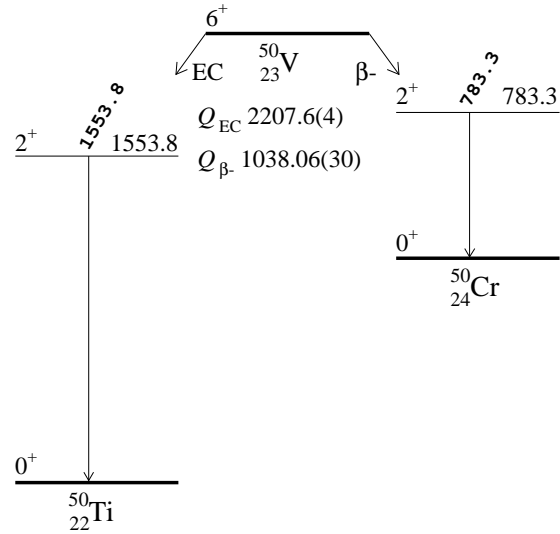


Figure 1: Decay scheme of  $^{50}\text{V}$ . No confirmed observation of the  $\beta^-$  decay of  $^{50}\text{V}$  to the  $2^+$  783.3 keV level of  $^{50}\text{Cr}$  has yet been performed.

Table 1: Half-lives of  $^{50}\text{V}$  relative to the electron capture to the  $2^+$  1553.8 keV excited level of  $^{50}\text{Ti}$  and  $\beta^-$  decay to the  $2^+$  783.3 keV excited level of  $^{50}\text{Cr}$ .

Reference (year)	Experimental technique	Half-life (yr)	
		Electron capture to $2^+$ 1553.8 keV	$\beta^-$ decay to $2^+$ 783.3 keV
[3] (1955)	Geiger counter,	$> 3.0 \times 10^{15}$	$> 3.0 \times 10^{14}$
[3] (1955)	Proportional counter		
[4] (1957)	Proportional counter, NaI(Tl) scintillation counter	$(4.0 \pm 1.1) \times 10^{14}$	$> 2.4 \times 10^{14}$
[5] (1958)	Proportional counter, NaI(Tl) scintillation counter	$(4.8 \pm 1.2) \times 10^{14}$	–
[6] (1961)	NaI(Tl) scintillation counter	$> 8.0 \times 10^{15}$	$> 1.2 \times 10^{16}$
[7] (1962)	NaI(Tl) scintillation counter	$(8.9 \pm 1.6) \times 10^{15}$	$(1.8 \pm 0.6) \times 10^{16}$
[8] (1966)	NaI(Tl) scintillation counter	$> 9.0 \times 10^{16}$	$> 6.9 \times 10^{16}$
[9] (1977)	Ge(Li) $\gamma$ spectrometry	$> 8.8 \times 10^{17}$	$> 7.0 \times 10^{17}$
[10] (1984)	HPGe $\gamma$ spectrometry	$(1.5_{-0.7}^{+0.3}) \times 10^{17}$	$> 4.3 \times 10^{17}$
[11] (1985)	HPGe $\gamma$ spectrometry	$(1.2_{-0.4}^{+0.8}) \times 10^{17}$	$> 1.2 \times 10^{17}$
[12] (1989)	HPGe $\gamma$ spectrometry	$(2.05 \pm 0.49) \times 10^{17}$	$(8.2_{-3.1}^{+13.1}) \times 10^{17}$
[13] (2011)	HPGe $\gamma$ spectrometry	$(2.29 \pm 0.25) \times 10^{17}$	$> 1.5 \times 10^{18}$
[14] (2019)	HPGe $\gamma$ spectrometry	$(2.67_{-0.18}^{+0.16}) \times 10^{17}$	$> 1.9 \times 10^{19}$
This work (2020)	HPGe $\gamma$ spectrometry	$(2.77_{-0.19}^{+0.20}) \times 10^{17}$	$> 8.9 \times 10^{18}$

In this work we report measurement of the  $^{50}\text{V}$  EC decay half-life and search for  $\beta^-$  decay of the nuclide using HPGe  $\gamma$  spectrometry of a 955 g vanadium sample.

## 2 EXPERIMENT

A disk-shaped sample of metallic vanadium with diameter of 100.1 mm and thickness of 19.9 mm with mass of  $955.21 \pm 0.02$  g, provided by Goodfellow Cambridge Ltd was used in the experiment. The vanadium disk was stored underground as soon as it was received by JRC-Geel in 2008 so that cosmogenic activation would be minimized. It was measured using an ultra low-background HPGe-detector system located 225 m underground in the laboratory HADES (Belgium). The detector system, named Pacman, consists of two HPGe-detectors facing each other [22]. The experiment was realized in two stages with different amount of Perspex in the inner volume of the lead/copper shield. At the start not all Perspex was available but due to time constraints it was judged beneficial to start the measurements anyhow. A schematic view of the two setups with HPGe detectors and the vanadium sample is shown in Fig. 2. The main characteristics of the HPGe detectors are presented in Table 2, more details can be found in [22, 23].

At the first stage of the experiment in setup I the vanadium sample was measured for 34.74 d, then the detectors were running for 38.16 d to measure background data without sample. The distance between the detectors Ge10 and Ge11 was 21 mm in setup I. The energy spectra accumulated with the vanadium sample and without sample in setup I are shown in Fig. 3.

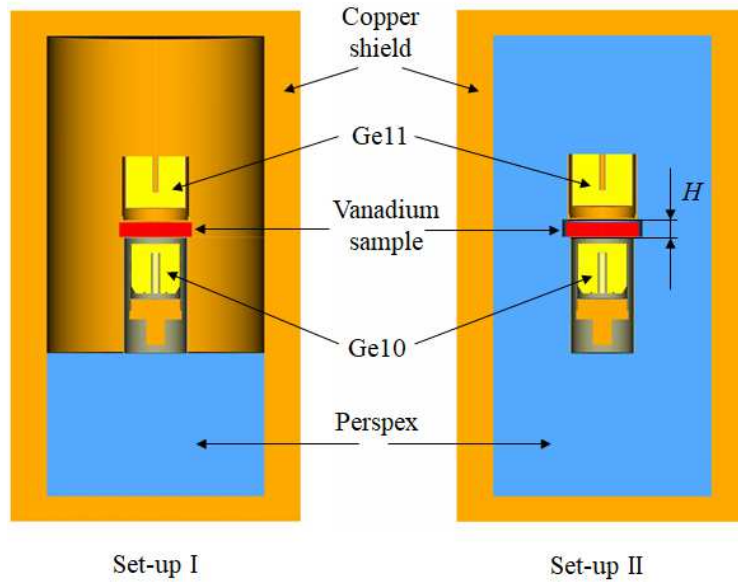


Figure 2: (Color online) Schematic view of the inner shield (Pb not shown) of the two low-background setups with HPGe detectors and vanadium sample.  $H$  denotes distance between the detectors Ge10 and Ge11, that can be adjusted taking into account a sample height.

Then the experiment was continued in setup II for 110.55 d with the vanadium sample and over 21.70 d to measure background without sample. The distance between the detectors Ge10 and Ge11 was 23 mm in setup II. Additional Perspex pieces were installed in setup II to minimize air inside so that to suppress background due to radon. The energy spectra gathered in setup II are shown in Fig. 4. The insertion of the Perspex details decreased background caused by  $^{222}\text{Rn}$  daughters. In particular the counting rates in the  $\gamma$ -ray peaks of  $^{214}\text{Bi}$  with energies 609.3 keV and 1764.5 keV were decreased by 3-5 times.

Table 2: Properties of the HPGe-detectors used in the present experiment. FWHM denotes the full width at half of maximum of  $\gamma$ -ray peak. HPAI = High Purity Aluminum. LB Cu = Low Background Copper

	Ge10	Ge11
Energy resolution (FWHM) at 1332 keV	1.7 keV	1.9 keV
Relative efficiency	62%	85%
Crystal mass	1040 g	1880 g
Endcap / Window material	HPAI / HPAI	LB Cu / LB Cu
Other characteristic	Submicron outer deadlayer	Inverted endcap (i.e. the window facing down)

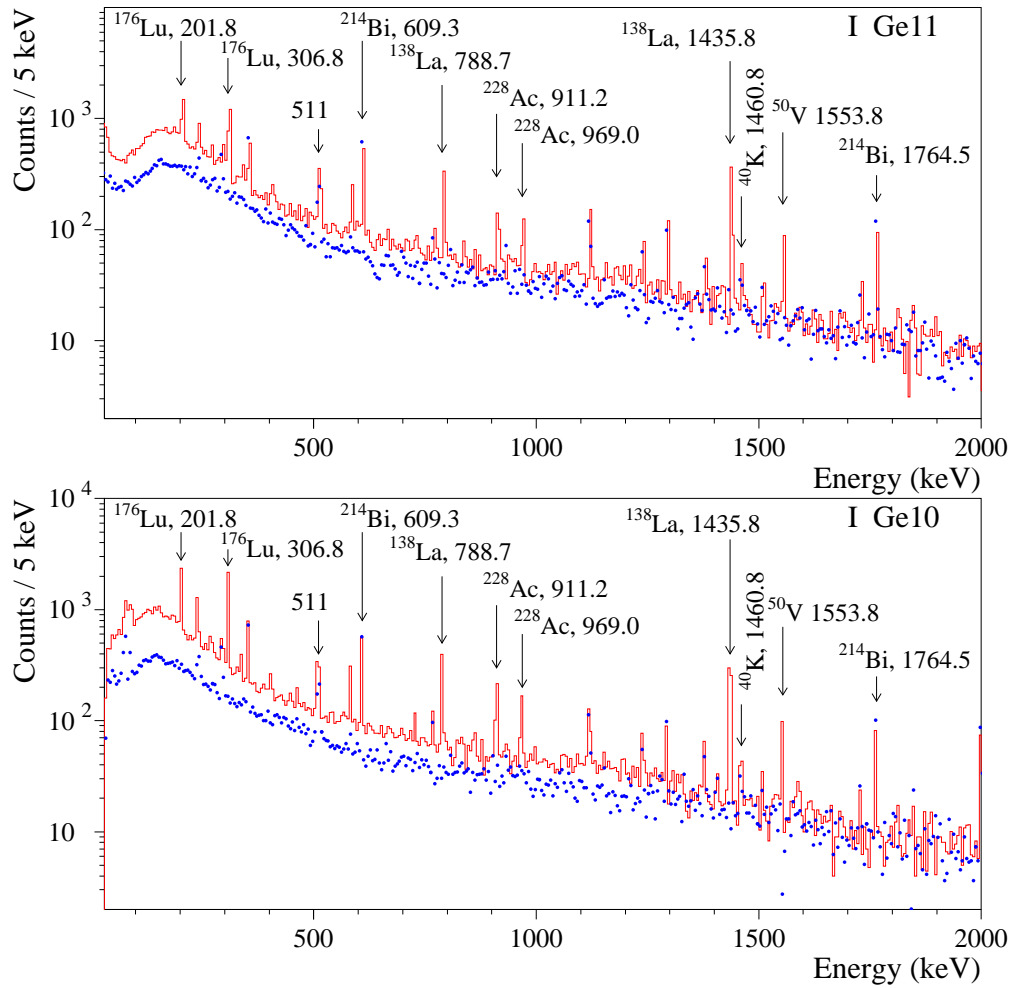


Figure 3: (Color online) The energy spectra accumulated in setup I with the vanadium sample for 34.74 days by detectors Ge11 (upper panel) and Ge10 (lower panel) (solid lines). The dotted histograms show background data measured without sample for 38.16 days by the detector Ge11 (upper panel) and Ge10 (lower panel). The background spectra are normalized on the time of measurements with the sample. Energy of  $\gamma$ -ray peaks are in keV.

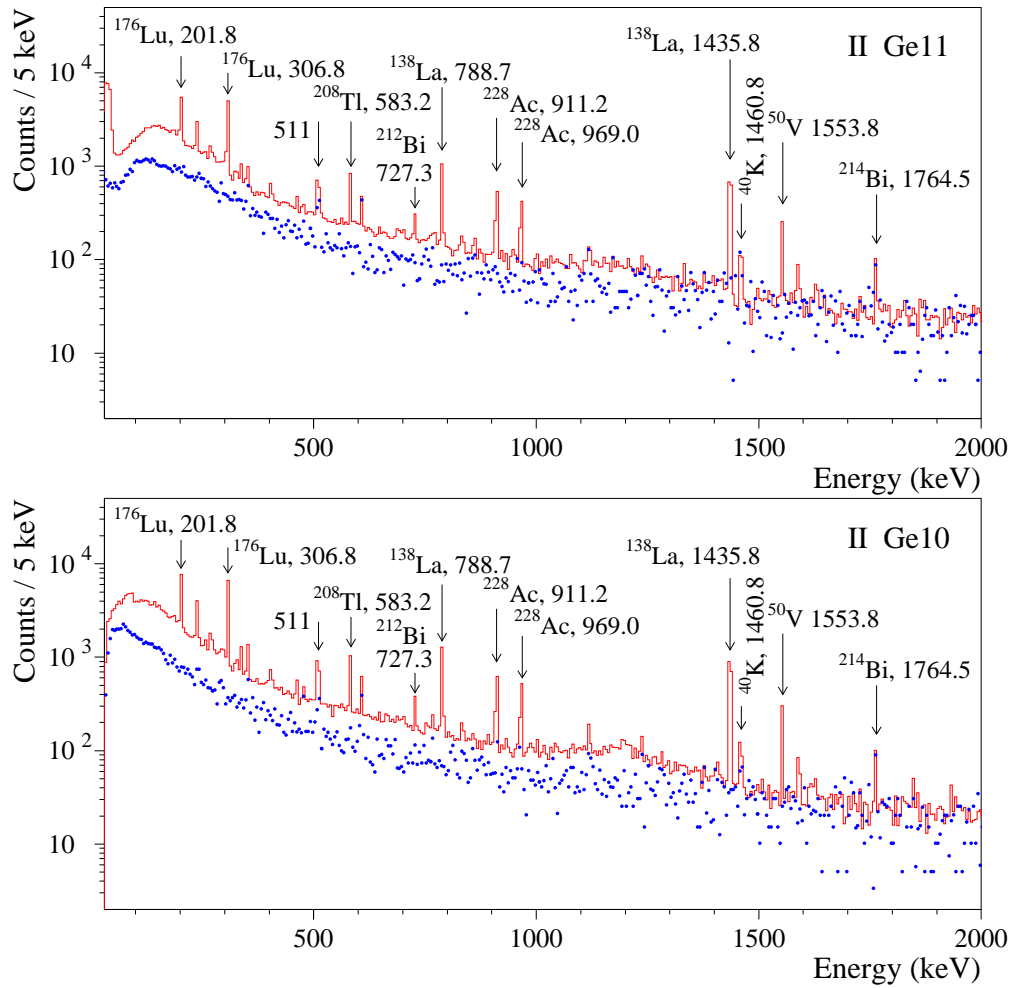


Figure 4: (Color online) The energy spectra accumulated in setup II with the vanadium sample by detectors Ge11 (for 110.55 d, upper panel) and Ge10 (110.55 d, lower panel) (solid lines). The dotted histograms show background data measured without sample by detector Ge11 (21.70 d, upper panel) and Ge10 (21.70 d, lower panel). The background spectra are normalized on the time of measurements with the sample. Energy of  $\gamma$ -ray peaks are in keV.

The energy spectra measured in the two setups are rather similar. The majority of the peaks could be assigned to  $^{40}\text{K}$  and nuclides of the  $^{232}\text{Th}$ ,  $^{235}\text{U}$ , and  $^{238}\text{U}$  decay chains. Besides, there are also clear peaks of  $^{138}\text{La}$  and  $^{176}\text{Lu}$  in the data taken with the vanadium sample that is evidence of the V-sample contamination by La and Lu. No unidentified peaks were observed.

The energy dependence of the energy resolution in the sum energy spectrum of the detectors Ge11 and Ge10 in setups I and II was estimated by using clear  $\gamma$ -ray peaks with energies  $E_\gamma = 201.8$  keV and  $306.8$  keV ( $^{176}\text{Lu}$ ),  $583.2$  keV ( $^{208}\text{Tl}$ ),  $609.3$  keV and  $1120.3$  keV ( $^{214}\text{Bi}$ ),  $788.7$  keV ( $^{138}\text{La}$ ),  $911.2$  keV ( $^{228}\text{Ac}$ ) as ( $E_\gamma$  is in keV):

$$\text{FWHM}(\text{keV}) = 0.72(9) + \sqrt{0.0019(8) \times E_\gamma} - 0.0003(2) \times E_\gamma. \quad (1)$$

## 3 RESULTS AND DISCUSSION

### 3.1 Radioactive impurities in the vanadium sample

Massic activities in the vanadium sample of  $^{40}\text{K}$ ,  $^{138}\text{La}$ ,  $^{176}\text{Lu}$ , daughters of the  $^{232}\text{Th}$ ,  $^{235}\text{U}$ , and  $^{238}\text{U}$  decay chains were calculated with the following formula:

$$A = (S_{\text{sample}}/t_{\text{sample}} - S_{\text{bg}}/t_{\text{bg}})/(\eta \varepsilon m), \quad (2)$$

where  $S_{\text{sample}}$  ( $S_{\text{bg}}$ ) is the area of a peak in the sample (background) spectrum;  $t_{\text{sample}}$  ( $t_{\text{bg}}$ ) is the time of the sample (background) measurement;  $\eta$  is the  $\gamma$ -ray emission intensity of the corresponding transition;  $\varepsilon$  is the full energy peak efficiency;  $m$  is the sample mass. The detection efficiencies were calculated with EGSnrc simulation package [24, 25], the events were generated homogeneously in the V sample. The calculations were validated using a liquid solution containing  $^{133}\text{Ba}$ ,  $^{134}\text{Cs}$ ,  $^{137}\text{Cs}$ ,  $^{60}\text{Co}$ , and  $^{152}\text{Eu}$ . The standard deviation of the relative difference between the simulations and the experimental data is 2.5% for  $\gamma$ -ray peaks in the energy interval 53 keV–1408 keV for Ge10 detector, and is 4% for  $\gamma$ -ray peaks in the energy interval 80 keV–1408 keV for Ge11 detector. The estimated massic activities of radioactive impurities in the vanadium sample are presented in Table 3.



Table 3: Radioactive contamination of the V sample measured by HPGe  $\gamma$ -ray spectrometry. The upper limits are given at 90% confidence level (C.L.), the reported uncertainties are the combined standard uncertainties.

Chain	Nuclide	Massic activity (mBq/kg)
	$^{40}\text{K}$	$3.7 \pm 1.2$
	$^{50}\text{V}$	$2.34 \pm 0.10$
	$^{138}\text{La}$	$18.7 \pm 0.2$
	$^{176}\text{Lu}$	$22.9 \pm 0.2$
$^{232}\text{Th}$	$^{228}\text{Ra}$	$16.1 \pm 0.6$
	$^{228}\text{Th}$	$12.7 \pm 1.0$
$^{235}\text{U}$	$^{235}\text{U}$	$\leq 4.9$
	$^{231}\text{Pa}$	$\leq 7.3$
	$^{227}\text{Ac}$	$11.4 \pm 0.5$
$^{238}\text{U}$	$^{234m}\text{Pa}$	$41 \pm 9$
	$^{226}\text{Ra}$	$\leq 0.5$

### 3.2 Electron capture decay of $^{50}\text{V}$ to the $2^+$ 1553.8 keV excited level of $^{50}\text{Ti}$

There is a clear peak with energy 1553.8 keV in all the energy spectra accumulated with the vanadium sample that can be ascribed to the electron capture decay of  $^{50}\text{V}$  to the  $2^+$  1553.8 keV level of  $^{50}\text{Ti}$ . The peak is absent in the background data. In order to estimate the half-life of  $^{50}\text{V}$  for the EC decay channel the sum energy spectrum of all the measurements with the vanadium sample was analyzed. A part of the spectrum in the energy region of interest is presented in Fig. 5. The exposure for  $^{50}\text{V}$  is  $(2.25 \pm 0.09) \times 10^{22}$  nuclei of  $^{50}\text{V} \times \text{yr}$ .

The spectrum was fitted in the energy interval (1520–1585) keV by a sum of a first order polynomial function (to describe the continuous distribution near the peak) and by Gaussian function (to describe the  $\gamma$ -ray peak). The fit with a very good value of  $\chi^2/\text{n.d.f.} = 100.2/126 = 0.795$  (where n.d.f. is number of degrees of freedom) returns the following peak parameters: energy of the peak is 1553.90(12) keV (in a good agreement with the table value 1553.768(8) keV [26]), the FWHM = 2.02(8) keV (again in a good agreement with the expected FWHM = 1.95 keV, see formula (1)), the area of the peak is 654(27) counts.

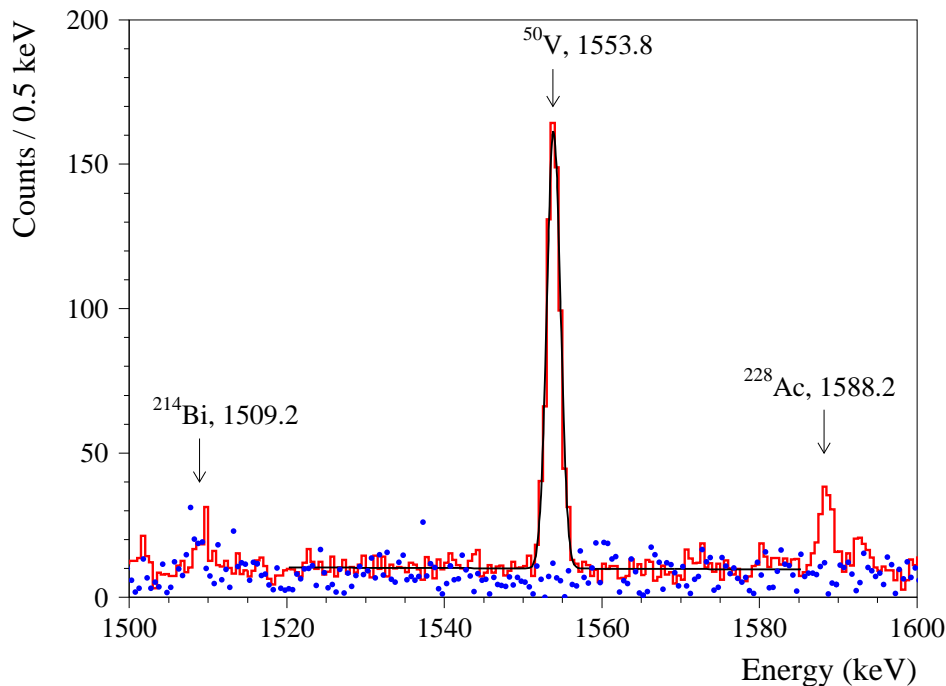


Figure 5: (Color online) The sum energy spectrum accumulated with the V sample in the vicinity of the 1553.8 keV  $\gamma$ -ray peak of  $^{50}\text{V}$ . The fit of the data by a sum of Gaussian peak (effect) and a straight line (background) is shown. The background energy spectrum, normalized on the time of measurements with the sample is shown by dots. Energy of  $\gamma$ -ray peaks are in keV.

The detection efficiencies for different detectors in the two setups for  $\gamma$ -ray quanta with energy 1553.8 keV were simulated with the help of the EGSnrc package [24, 25]. The detection efficiencies are given in Table 4.

The half-life of  $^{50}\text{V}$  relative to the electron capture to the  $2^+$  1553.8 keV level of  $^{50}\text{Ti}$  ( $T_{1/2}$ ) was calculated by using the following formula:

Table 4: Monte Carlo simulated full energy peak detection efficiencies for 1553.8 keV  $\gamma$ -ray quanta, live-times of the measurements, areas of the 1553.8 keV peak,  $^{50}\text{V}$  half-life values ( $T_{1/2}^{\text{EC}}$ ) for different detectors in the two setups. The standard statistical errors of the detection efficiencies, areas of the peak and half-life values are given.

Setup	Detector	Detection efficiency	Live-time of measurement (s)	1553.8 keV peak area	$T_{1/2}^{\text{EC}} \times 10^{17}$ (yr)
I	Ge11	0.011324(25)	3000651	79(9)	$2.67^{+0.34}_{-0.27}$
I	Ge10	0.012508(25)	3002755	83(10)	$2.81^{+0.38}_{-0.30}$
II	Ge11	0.010607(22)	9551494	220(16)	$2.86^{+0.22}_{-0.19}$
II	Ge10	0.012536(25)	9551342	270(17)	$2.75^{+0.18}_{-0.16}$

$$T_{1/2} = N \ln 2 \sum (\eta_i t_i) / S \quad (3)$$

where  $N$  is number of  $^{50}\text{V}$  nuclei in the sample [ $N = 2.823(113) \times 10^{22}$ ],  $\eta_i$  and  $t_i$  are detection efficiencies and times of measurement for the two detectors in the two setups (given in Table 4),  $S$  is area of the peak with energy 1553.8 keV obtained by the fit of the data of the sum energy spectrum shown in Fig. 5 ( $S = 654 \pm 27$  counts). By using these data the half-life of  $^{50}\text{V}$  has been calculated as  $T_{1/2}^{\text{EC}} = [2.774^{+0.119}_{-0.110}(\text{stat})] \times 10^{17}$  yr.

In addition to the  $\approx 0.2\%$  statistical uncertainty of the Monte Carlo simulated detection efficiency we conservatively assess a  $4\%^2$  systematic uncertainty on the calculated detection efficiency of the detector system to the 1553.8 keV  $\gamma$ -ray quanta. An indirect confirmation of a rather small systematic of the detection efficiency can be seen in Table 4 and Fig. 6 where the  $T_{1/2}^{\text{EC}}$  values determined from the data of measurements with two different detectors in setups I and II are presented. The difference between the half-life values is well within the statistical errors, that does demonstrate stability of the half-life result and its independence neither on the detector nor the experimental setup.

Variation of the energy interval of fit from 1520–1540 keV (starting point) to 1570–1585 keV (final point), changes  $T_{1/2}^{\text{EC}}$  up to 1.1%. Finally, we account 4.0% for uncertainty in the number of  $^{50}\text{V}$  nuclei in the sample due to the accuracy of the representative isotopic abundance of the isotope [1]. The summary of the systematic uncertainties is given in Table 5.

Table 5: Estimated systematic uncertainties of the EC decay half-life (%).

Number of $^{50}\text{V}$ nuclei	4.0
Monte Carlo statistics	0.2
Monte Carlo systematic	4.0
Interval of fit	1.1
Total systematic uncertainty	5.8

---

<sup>2</sup>See discussion of the difference between the simulations and the experimental data used for the validation of the simulations in Sec. 3.1.

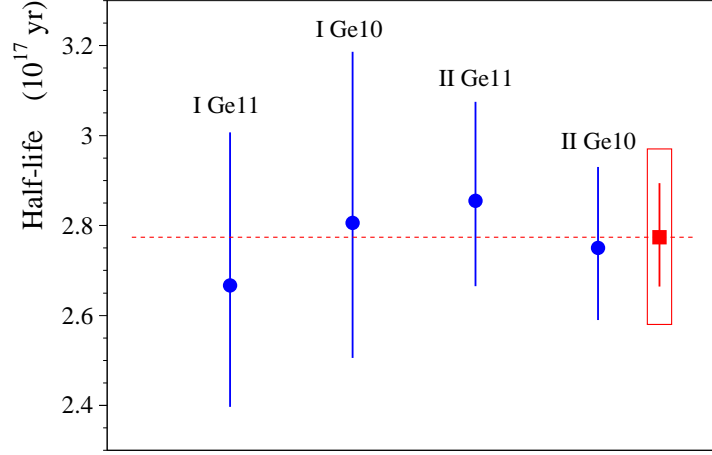


Figure 6: (Color online) Half-life of  $^{50}\text{V}$  relative to the electron capture to the  $2^+$  1553.8 keV level of  $^{50}\text{Ti}$  determined from the data of measurements with the detectors Ge10 and Ge11 in setups I and II (points, see also Table 4). The final result of the present work, obtained by analysis of the sum spectrum of the detectors in the two setups, is shown by a square. The error bars represent the statistical errors, while the box around the final value show the errors calculated by summing in quadrature the statistical and systematic uncertainties.

Adding all the systematic uncertainties in quadrature, the half-life is

$$T_{1/2}^{\text{EC}} = [2.77^{+0.12}_{-0.11}(\text{stat}) \pm 0.16(\text{syst})] \times 10^{17} \text{ yr.}$$

By summing in quadrature the statistical and systematic uncertainties the half-life of  $^{50}\text{Ti}$  relative to the electron capture to the  $2^+$  1553.8 keV excited level of  $^{50}\text{Ti}$  is

$$T_{1/2}^{\text{EC}} = (2.77^{+0.20}_{-0.19}) \times 10^{17} \text{ yr.}$$

A historical perspective of half-life of  $^{50}\text{V}$  is presented in Fig. 7. It is interesting to note that early experiments claimed too short half-lives. That can be explained, first of all, by utilization of rather low energy resolution detectors like proportional counters and NaI(Tl) scintillation counters (see Table 1). Other possible reasons for obtaining a too short half-life can be using nonpure samples, high background with possible interferences of  $\gamma$  rays of different origin (including cosmogenic activation, since most of the earlier experiments were performed in laboratories on the ground level), less good electronics, stability problems of long measurements. The latter point is especially crucial in conditions of a poor energy resolution.

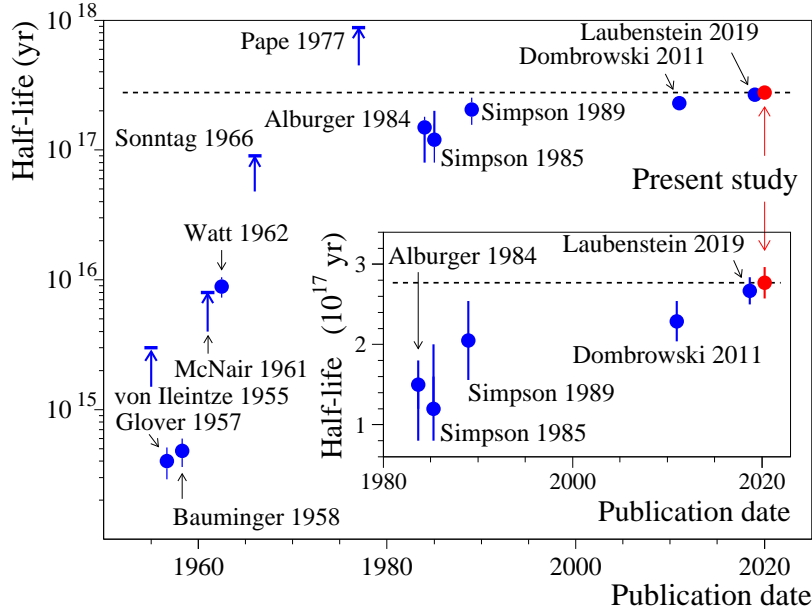


Figure 7: (Color online) A historical perspective of half-life of  $^{50}\text{V}$  relative to the EC decay as a function of the publication date (references to the publications are as follows: von Ileintze 1955: [3], Glover 1957: [4], Bauminger 1958: [5], McNair 1961: [6], Watt 1962: [7], Sonntag 1966: [8], Pape 1977: [9], Alburger 1984: [10], Simpson 1985: [11], Simpson 1989: [12], Dombrowski 2011: [13], Laubenstein 2019: [14]). The results are presented by dots, while the limits are shown by arrows. The early positive claims of EC decay in  $^{50}\text{V}$  with too short half-lives were obtained with low resolution detectors: proportional and NaI(Tl) scintillation counters [4, 5], NaI(Tl) scintillation counter [7]. The half-lives measured with the help of HPGe detectors in works [10, 11, 12, 13, 14] and in the present study are in a reasonable agreement.

### 3.3 Limit on $\beta^-$ decay of $^{50}\text{V}$ to the $2^+$ 783.3 keV excited level of $^{50}\text{Cr}$

There is no peak with energy  $\approx 783$  keV in the sum energy spectrum that can be interpreted as  $\beta^-$  decay of  $^{50}\text{V}$  to the  $2^+$  783.3 keV excited level of  $^{50}\text{Cr}$ . Thus, we have set a lower half-life limit on the decay with the following formula:

$$\lim T_{1/2} = N \ln 2 \sum (\eta_i t_i) / \lim S, \quad (4)$$

where  $N$  is the number of  $^{50}\text{V}$  nuclei in the sample,  $\eta_i$  and  $t_i$  are detection efficiencies (for 783.3 keV  $\gamma$ -ray quanta) and times of measurement for the two detectors in the two setups, and  $\lim S$  is the number of events of the effect searched for which can be excluded at a given confidence level. The detection efficiencies for different detectors were simulated with the help of the EGSnrc package [24, 25].

To estimate the value of  $\lim S$  the sum energy spectrum with exposure  $(2.25 \pm 0.09) \times 10^{22}$  nuclei of  $^{50}\text{V} \times \text{yr}$  was fitted by a background model that includes the effect searched for (a peak centered at 783.3 keV with a fixed FWHM = 1.69 keV), several Gaussian peaks to describe background  $\gamma$ -ray peaks of  $^{138}\text{La}$ ,  $^{212}\text{Bi}$  (daughter of the  $^{228}\text{Th}$  subchain from the  $^{232}\text{Th}$  chain),  $^{214}\text{Bi}$  and  $^{214}\text{Pb}$  (daughters of  $^{226}\text{Ra}$  from the  $^{238}\text{U}$  chain),  $^{228}\text{Ac}$  (daughter of the  $^{228}\text{Ra}$  subchain from the  $^{232}\text{Th}$  chain),  $^{234m1}\text{Pa}$  (daughter of  $^{238}\text{U}$ ), and a straight line to describe the continuous background. While the areas and positions of intensive peaks (766.4 keV of  $^{234m1}\text{Pa}$ , 768.4 keV of  $^{214}\text{Bi}$ , 785.4 keV of  $^{212}\text{Bi}$ , 788.7 keV of  $^{138}\text{La}$ , 795.0 keV of  $^{228}\text{Ac}$ ) were free parameters of the fit, the areas and positions of weak peaks (772.3 keV and 782.1 keV of  $^{228}\text{Ac}$ , 786.0 keV of  $^{214}\text{Pb}$ , 786.3 keV of  $^{234m1}\text{Pa}$ , 786.4 keV of  $^{214}\text{Bi}$ ), superimposed on nearby intensive peaks, were fixed taking into account their relative intensities in the sub-chains. All the peak widths were fixed taking into account the dependence of the energy resolution on energy of  $\gamma$ -ray quanta (1).

The best fit, achieved in the energy interval 761–818 keV with  $\chi^2/\text{n.d.f.} = 0.815$ , returned an area  $3.3 \pm 15.5$  counts in an expected 783.3 keV peak that is no evidence of the effect searched for.<sup>3</sup> The fit and excluded peak are shown in Fig. 8. According to [27] we took  $\lim S = 28.7$  counts and, taking into account the detection efficiencies to 783.3 keV  $\gamma$ -ray quanta (given in Table 6), obtain the following limit on the  $\beta^-$  decay of  $^{50}\text{V}$  to the  $2^+$  783.3 keV excited level of  $^{50}\text{Cr}$ :

$$T_{1/2}^\beta \geq 8.9 \times 10^{18} \text{ yr at 90\% C.L.}$$

---

<sup>3</sup>The estimations of the  $\lim S$  value includes only the statistical uncertainty, and any systematic contributions have not been considered.

Table 6: Monte Carlo simulated full absorption peak detection efficiencies for 783.3 keV  $\gamma$ -ray quanta for different detectors in the two setups.

Setup	Detector	Detection efficiency
I	Ge11	0.014986
I	Ge10	0.018497
II	Ge11	0.014140
II	Ge10	0.018481

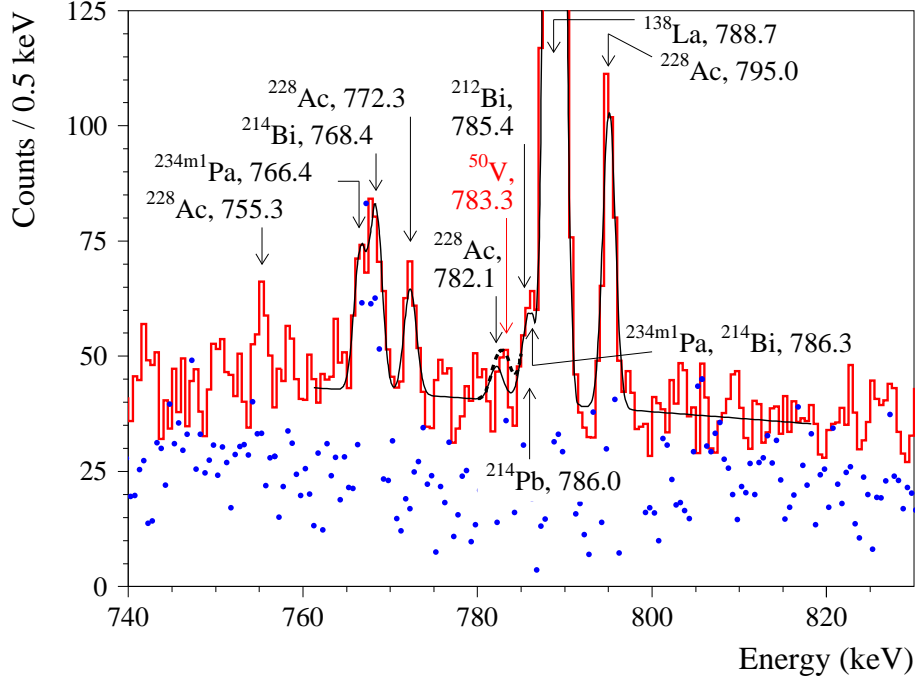


Figure 8: (Color online) Part of the sum energy spectrum accumulated with the vanadium sample in the vicinity of the expected  $\beta^-$  decay 783.3 keV  $\gamma$ -ray peak. Fit of the data by several  $\gamma$ -ray peaks and by a straight line to describe the continuous background is shown by solid line, while an excluded peak expected in the  $\beta^-$  decay of  $^{50}\text{V}$  is presented by dashed line. The background energy spectrum, normalized on the time of measurements with the sample is shown by dots. Energy of  $\gamma$ -ray peaks are in keV.

The limit is approximately two times weaker than the limit  $T_{1/2}^{\beta} \geq 1.9 \times 10^{19}$  yr reported in [14]. The sensitivity of the present experiment is lower mainly due to a rather high radioactive contamination of the vanadium sample that produce background in the region of interest.

Therefore, an advanced experiment should utilize a radio-pure vanadium sample. A possibility of a deep purification of vanadium from radioactive impurities has been demonstrated in [14]. Thus, aiming to estimate requirements to experiments able to detect the decay, we assume a level of background already achieved in setup II without sample (see Fig. 4). We consider two vanadium containing samples: a metallic vanadium of the natural isotopic composition with the sizes and geometry the same as in the present experiment, and a second one in form of vanadium oxide ( $\text{V}_2\text{O}_5$ ), enriched in the isotope  $^{50}\text{V}$  to 50%. We assume the bulk density of enriched vanadium oxide sample to be 0.5 of the solid  $\text{V}_2\text{O}_5$  density ( $3.36 \text{ g/cm}^3$ ). To get the same number of  $^{50}\text{V}$  nuclei ( $2.82 \times 10^{22}$ ), the size of the enriched sample was chosen to be  $\varnothing 50 \times 2.57$  mm, with a distance between the detectors  $H = 3$  mm. Expected background counting rates and the Monte Carlo simulated detection efficiencies of the Pacman setup with the samples are given in Table 7.



Table 7: Characteristics of experimental setups to estimate sensitivity to the  $\beta^-$  decay of  $^{50}\text{V}$ .  $H$  denotes distance between the detectors Ge10 and Ge11 (see Fig. 2),  $\text{BG}^{\text{det}}$  is background counting rate of the detectors (achieved in setup II without sample),  $\text{BG}^{\text{EC}}$  is Monte Carlo simulated counting rate due to the EC decay of  $^{50}\text{V}$ ,  $\eta_{783}$  is detection efficiency to  $\gamma$ -ray quanta with energy 783.3 keV.

Sample, Experimental geometry	$\text{BG}^{\text{det}}$ (counts/day/keV)		$\text{BG}^{\text{EC}}$ (counts/day/keV)		$\eta_{783}$	
	Ge10	Ge11	Ge10	Ge11	Ge10	Ge11
V metal, natural isotopic composition $\varnothing 100 \times 20$ mm, $H = 21$ mm	0.1291(8)	0.1176(8)	0.0074	0.0065	0.01850	0.01499
$\text{V}_2\text{O}_5$ , enriched in $^{50}\text{V}$ to 50% $\varnothing 50 \times 2.57$ mm, $H = 3$ mm	0.1291(8)	0.1176(8)	0.0143	0.0106	0.05496	0.03716

The background of the detectors dominates in the experimental conditions, with the contribution from the EC process in  $^{50}\text{V}$  an order of magnitude smaller. While the assumed enriched source contains the same number of  $^{50}\text{V}$  nuclei as the metallic one with the natural isotopic composition, the detection efficiency with the enriched source is about three times higher. As a result, an experiment with enriched source has a higher sensitivity [see Fig. 9, (a)]. Moreover, utilization of enriched  $^{50}\text{V}$  would allow to observe clearly the  $\beta^-$  decay of  $^{50}\text{V}$  (assuming the theoretically predicted half-life  $T_{1/2}^{\beta^-} = 2 \times 10^{19}$  yr [16]) with a  $3\sigma$  accuracy over about 200 d of data taking, while an experiment utilizing a V-sample of natural isotopic composition needs more than three years to detect the process with a similar accuracy (see Fig. 9, (b)).

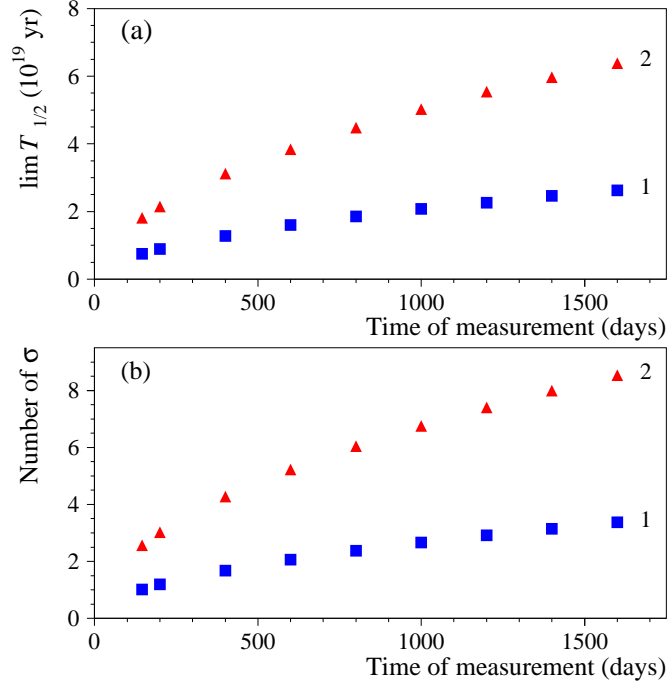


Figure 9: (Color online) Sensitivity of possible experiments to detect the  $\beta^-$  decay of  $^{50}\text{V}$  [expressed as: (a) a lower half-life limit at 90% C.L.; (b) a number of  $\sigma$  for accuracy of the expected 783.3 keV peak area, assuming the half-life  $T_{1/2}^{\beta^-} = 2 \times 10^{19}$  yr] depending on time of measurement in two experimental conditions: (1) in the geometry of the present experiment (with a V-sample  $\varnothing 100 \times 20$  mm and distance between the detectors Ge10 and Ge11  $H = 21$  mm); (2) with a  $\text{V}_2\text{O}_5$ -sample enriched in the isotope  $^{50}\text{V}$  to 50% with sizes  $\varnothing 50 \times 2.57$  mm and  $H = 3$  mm. Only background without sample together with contribution due to the EC decay of  $^{50}\text{V}$  are assumed.

## 4 CONCLUSIONS

The half-life of  $^{50}\text{V}$  relative to the EC to the  $2^+$  1553.8 keV level of  $^{50}\text{Ti}$  is measured as  $T_{1/2}^{\text{EC}} = (2.77_{-0.19}^{+0.20}) \times 10^{17}$  yr. The value is in agreement with the result of the recent experiment [14] and the theoretical predictions [16]. The  $\beta^-$  decay of  $^{50}\text{V}$  to the  $2^+$  783.3 keV level of  $^{50}\text{Cr}$  is limited as  $T_{1/2}^{\beta} \geq 8.9 \times 10^{18}$  yr at 90% C.L. The limit is about 2 times weaker than that set in the work [14]. Further improvement of the experiment sensitivity could be achieved by utilization of highly purified vanadium samples. Moreover, using of a sample enriched in  $^{50}\text{V}$  would allow detection of the  $\beta^-$  decay. The accuracy of  $T_{1/2}^{\text{EC}}$  will also be improved with a source enriched in  $^{50}\text{V}$  both thanks to improvement of statistics and reduction of the uncertainty in the  $^{50}\text{V}$  isotopic abundance.

## 5 ACKNOWLEDGMENTS

This work received support from the EC-JRC open access scheme EUFRAT under Horizon-2020, project No. 22-14. D.V.K. and O.G.P. were supported in part by the project “Investigation of double beta decay, rare alpha and beta decays” of the program of the National Academy of Sciences of Ukraine “Laboratory of young scientists” (the grant number 0120U101838). F.A.D. greatly acknowledges the Government of Ukraine for the quarantine measures that have been taken against the Coronavirus disease 2019 that substantially reduced much unnecessary bureaucratic work.

## References

- [1] J. Meija *et al.*, Isotopic compositions of the elements 2013 (IUPAC Technical Report), Pure Appl. Chem. 88 (2016) 293.
- [2] M. Wang *et al.*, The AME2016 atomic mass evaluation, Chin. Phys. C 41 (2017) 030003.
- [3] J. von Ileintze, Zur Frage der natürlichen Radioaktivität des  $\text{V}^{50}$ ,  $\text{In}^{113}$  und  $\text{Te}^{123}$ , Z. Naturforschung 10a (1955) 77.
- [4] R. N. Glover and D. E. Watt, A search for natural radioactivity in vanadium, Philos. Mag. 2 (1957) 697.
- [5] E. R. Bauminger and S. G. Cohen, Natural radioactivity of  $\text{V}^{50}$  and  $\text{Ta}^{180}$ , Phys. Rev. 110 (1958) 953.
- [6] A. McNair, The half-life of vanadium-50, Philos. Mag. 6 (1961) 559.
- [7] D. E. Watt and R. L. G. Keith, The half-life of  $^{50}\text{V}$ , Nucl. Phys. 29 (1962) 648.
- [8] Ch. Sonntag and K. O. Münnich, A search for the decay of vanadium-50 with a low-level gamma-spectrometer, Z. Physik 197 (1966) 300.
- [9] A. Pape, S. M. Refaei, and J. C. Sens,  $^{50}\text{V}$  half-life limit, Phys. Rev. C 15 (1977) 1937.

- [10] D. E. Alburger, E. K. Warburton, and J. B. Cumming, Decay of  $^{50}\text{V}$ , Phys. Rev. C 29 (1984) 2294.
- [11] J. J. Simpson, P. Jagam, and A. A. Pilt, Electron capture decay rate of  $^{50}\text{V}$ , Phys. Rev. C 31 (1985) 575.
- [12] J. J. Simpson, P. Moorhouse, and P. Jagam, Decay of  $^{50}\text{V}$ , Phys. Rev. C 39 (1989 ) 2367.
- [13] H. Dombrowski, S. Neumaier, and K. Zuber, Precision half-life measurement of the 4-fold forbidden  $\beta$  decay of  $^{50}\text{V}$ , Phys. Rev. C 83 (2011) 054322.
- [14] M. Laubenstein, B. Lehnert, S. S. Nagorny, S. Nisi, and K. Zuber, New investigation of half-lives for the decay modes of  $^{50}\text{V}$ , Phys. Rev. C 99 (2019) 045501.
- [15] P. Belli *et al.*, Experimental searches for rare alpha and beta decays, Eur. Phys. J. A 55 (2019) 140.
- [16] M. Haaranen, P. C. Srivastava, J. Suhonen, and K. Zuber,  $\beta$ -decay half-life of  $^{50}\text{V}$  calculated by the shell model, Phys. Rev. C 90 (2014) 044314.
- [17] J. Barea, J. Kotila, and F. Iachello, Nuclear matrix elements for double- $\beta$  decay, Phys. Rev. C 87 (2013) 014315.
- [18] S. Dell’Oro, S. Marcocci, and F. Vissani, New expectations and uncertainties on neutrinoless double beta decay, Phys. Rev. D 90 (2014) 033005.
- [19] J. T. Suhonen, Impact of the quenching of  $g_A$  on the sensitivity of  $0\nu 2\beta$  experiments, Phys. Rev. C 96 (2017) 055501.
- [20] J. T. Suhonen, Value of the axial-vector coupling strength in  $\beta$  and  $\beta\beta$  decays: A review, Front. in Phys. 5 (2017) 55.
- [21] H. Ejiri, J. Suhonen, and K. Zuber, Neutrino-nuclear responses for astro-neutrinos, single beta decays and double beta decays, Phys. Rep. 797 (2019) 1.
- [22] G. Lutter *et al.*, A new versatile underground gamma-ray spectrometry system, Appl. Radiat. Isot. 81 (2013) 81.
- [23] M. Hult *et al.*, Comparison of background in underground HPGe-detectors in different lead shield configurations, Appl. Radiat. Isot. 81 (2013) 103.
- [24] I. Kawrakow *et al.*, The EGSnrc Code System: Monte Carlo Simulation of Electron and Photon Transport. Technical Report No. PIRS-701, National Research Council Canada (2017).
- [25] G. Lutter, M. Hult, G. Marissens, H. Stroh, and F. Tzika, A gamma-ray spectrometry analysis software environment, Appl. Rad. Isot. 134 (2018) 200.
- [26] J. Chen and B. Singh, Nuclear Data Sheets for A=50, Nucl. Data Sheets 157 (2019) 1.
- [27] G. J. Feldman and R. D. Cousins, Unified approach to the classical statistical analysis of small signals, Phys. Rev. D 57 (1998) 3873.